

E6-2022-60

A. Kh. Inoyatov^{1,2}, D. Vénos³, A. Kovalík^{2,3}

EXPERIMENTAL DETERMINATIONS
OF THE ENERGY OF THE 9.4 keV
($M1 + E2$) NUCLEAR TRANSITION IN ^{83}Kr
AND THE Kr ELECTRON BINDING ENERGIES
IN DIFFERENT MATRICES BY **ICES** METHOD

Submitted to “Physica Scripta”

¹ Nuclear Physics Institute of the AS RUz, township Ulugbek, 100214
Tashkent, Republic of Uzbekistan

² Joint Institute for Nuclear Research, 141980 Dubna, Moscow Region,
Russian Federation

³ Nuclear Physics Institute of the AS CR, CZ-25068 Řež near Prague,
Czech Republic

Инояттов А. Х., Венос Д., Ковалик А.

E6-2022-60

Экспериментальное определение энергии ядерных переходов ($M1 + E2$) 9,4 кэВ в ^{83}Kr и энергий связи электронов Кг в различных матрицах методом спектроскопии электронов внутренней конверсии

Методом спектроскопии электронов внутренней конверсии измерена энергия ядерного перехода ($M1 + E2$) 9,4 кэВ в ^{83}Kr . Измеренное значение 9406,3(5) эВ согласуется в пределах 1σ с принятым средневзвешенным значением 9405,9(2) эВ, установленным из данных предыдущих измерений. По нашим данным, разность энергий между ядерными переходами 32,1 и 9,4 кэВ в ^{83}Kr составляет 22745,3(2) эВ. Также измерены энергии связи электронов в K , L и $M_{1,2,3}$ подоболочках Кг, имплантированного в поликристаллическую матрицу Pt. Установленные значения энергии связи в среднем на 11,6(4) и 1,7(6) эВ меньше, чем для свободных атомов криптона и ^{83}Kr , образующегося в слое ^{83}Rb , испаренного на поверхность алюминиевой подложки, соответственно, и больше на 2,9(2) эВ, чем для ^{83}Kr в слое ^{83}Rb , испаренного на поверхность подложки из поликристаллической платины.

Работа выполнена в Лаборатории ядерных проблем им. В. П. Дзелепова ОИЯИ.

Препринт Объединенного института ядерных исследований. Дубна, 2022

Inoyatov A. Kh., Vénos D., Kovalík A.

E6-2022-60

Experimental Determinations of the Energy of the 9.4 keV ($M1 + E2$) Nuclear Transition in ^{83}Kr and the Kr Electron Binding Energies in Different Matrices by ICES Method

The energy value of 9406.3(5) eV was determined for the 9.4 keV ($M1 + E2$) nuclear transition in ^{83}Kr by the internal conversion electron spectroscopy method. This value agrees within 1σ with the most precise ones of the previous measurements, and their weighted mean amounts to 9405.9(2) eV. A value of 22745.3(2) eV was obtained directly from our experimental data for the energy difference of the 32.1 and 9.4 keV transitions in ^{83}Kr . Electron binding energies (related to the Fermi level) on the K , L , and $M_{1,2,3}$ subshells of Kr implanted into the polycrystalline Pt matrix were also derived. They were found to be lower by the weighted mean values of 11.6(4) and 1.7(6) eV than those for free Kr atoms and for Kr in the evaporated ^{83}Rb layer on the Al backing, respectively, and higher by the weighted mean value of 2.9(2) eV than the binding energies in Kr in an evaporated layer on the polycrystalline Pt backing.

The investigation has been performed at the Dzhelapov Laboratory of Nuclear Problems, JINR.

Preprint of the Joint Institute for Nuclear Research. Dubna, 2022

INTRODUCTION

Till now, several experimental energy determinations of the 9.4 keV ($M1 + E2$) nuclear transition depopulating the lowest excited state $7/2^+$ in ^{83}Kr were performed. The present adopted value of 9405.7(6) eV [1] was obtained as a weighted mean of the three most precise results. Two of them, namely, 9396(3) eV [2] and 9405.9(8) eV [3], were obtained by the Internal Conversion Electron Spectroscopy (ICES). In the former measurement [2], studied ^{83}Rb sources were prepared by vacuum evaporation on Al backings, while in the latter one [3] a condensed ^{83m}Kr source was used. The third value of 9405.8(3) eV was obtained [4] from photon spectrometry measurements using an $^{83}\text{Rb}/^{83m}\text{Kr}$ source. The determination of the energy value of 9396(3) eV [2] was based on: i) the measured energy differences between the K conversion line of the 32.1 keV transition in ^{83}Kr and the L_1 , L_2 , L_3 , M_1 , and N_1 conversion electron lines of the 9.4 keV transition, ii) a preferred energy value of the 32.1 keV transition, and iii) a set of differences of the Kr electron binding energies between the K shell and the above-mentioned L_1 , L_2 , L_3 , M_1 , and N_1 subshells. The main advantage of this method is usage of relative quantities of both the electron binding energies (a way of elimination of the unknown value of the work function for the given solid-state backing as the available data for Kr are referenced to the vacuum level) and the measured conversion line positions (minimization of the possible inaccuracy in the calibration of the absolute energy scale of the electron spectrometer used). Because of still unclear considerable difference (exceeding 3 standard deviations σ) of the value [2] from the other two [3, 4] and its substantially lower precision, we decided to perform a new ICES measurement using an approach similar to that in the work [2]. To ensure the most defined and stable physicochemical environment of ^{83}Kr atoms, we opted to use $^{83}\text{Sr}/^{83}\text{Rb}/^{83m}\text{Kr}$ sources prepared by an ion-implantation of ^{83}Sr into Pt matrices. Moreover, an $^{83}\text{Rb}/^{83m}\text{Kr}$ source produced by thermal evaporation in vacuum of ^{83}Rb on a Pt backing was also used in the investigation. The aim was to study also influence of the physicochemical solid state surroundings on the Kr electron binding energies.

1. EXPERIMENTAL

1.1. Source Preparations. The strontium isotopes were produced on the Phasotron particle accelerator at the JINR, Dubna, and were also separated there on a mass separator with subsequent implantation into a polycrystalline

platinum foil at an energy of 30 keV. A piece of the foil including only atoms with mass $A = 83$ was cut out and used for electron spectrum measurements. The size of the “radioactive” spot was about 2×2 cm. Some other details can be found in Refs. [5, 6].

The computer code SRIM [7] for Monte Carlo simulation of ion implantations was used to estimate the depth distribution of the implanted ^{83}Sr atoms. Basic real conditions of the implantation were taken into account in the simulations, namely, the zero ion incident angle (relative to the source foil normal), polycrystalline structure of the platinum and adsorbed surface contamination layer represented by an additional 3-nm-thick pure carbon layer on the foil surfaces [8]. As can be seen from Fig. 1, the average ion range reaches 8.8 nm (including the above-mentioned 3-nm-thick contamination layer). Moreover, a portion of about 5% of the incident ^{83}Sr ions were found in the surface contamination layer. (It should be noted that this fact was experimentally proved [9, 10] in the case of the implantation of the ^{83}Rb ions into a similar Pt foil.) The contamination layer represents different physicochemical surrounding for ^{83}Sr ions than does the bulk foil material. During transfer of the prepared source to the electron spectrometer, the ^{83}Sr ions in the contamination layer were exposed to air and, as a result, they were mostly bound with oxygen in all possible forms (oxides, hydroxides, carbonates, hydrocarbonates, etc.) and had the oxidation number +2. The daughter ^{83}Rb atoms were most likely stabilized in the ^{83}Sr matrix of the contamination layer. The ^{83}Rb ions were thus bound with oxygen atoms in anions of all possible relevant forms (O^{2-} , OH^- , CO_3^{2-} , HCO_3^- , etc.). Contrary to ^{83}Sr , they had the oxidation number +1. This conclusion is supported by similar experiments from the past performed, e.g.,

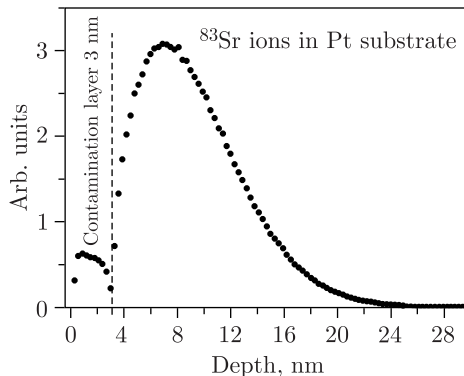


Fig. 1. The depth distributions of the ^{83}Sr ions implanted at 30 keV into the high-purity polycrystalline platinum foil as calculated by the computer code SRIM [7]. The depth values on the x axis (represented by the foil normal) also include the thickness of the adsorbed contamination layer on the foil surface represented in the simulations by a pure carbon layer 3 nm thick. The average range of the ^{83}Sr ions in the foil amounts to 8.8 nm

with ^{99m}Tc (see, e.g., [11–13]). It should be noted that the contamination layer was not removed from the source surface before our electron spectrum measurements.

A preparation of the evaporated ^{83}Rb source started by a deposition of the rubidium fraction (obtained from the above irradiated material) on a Ta evaporation boat (annealed at about 1300°C) and its subsequent desiccation. Afterwards possible volatile organic compounds were removed from the deposit by preheating the Ta boat at around 800°C for about 30 s. During the procedure, the source backing was shielded. Evaporation of ^{83}Rb compounds took place at 1400°C for several seconds. Throughout, the source backing with the mask rotated around their common axis at a speed of 3000 turns/min to improve homogeneity of the evaporated layer. More details on the preparation techniques of similar radioisotopes can be found, e.g., in Ref. [6]. The oxidation number of the ^{83}Rb ions should be similar to the case of the above-discussed contamination layer on the implanted source.

1.2. Measurements and Energy Calibration. The combined electrostatic electron spectrometer [14] (see Fig. 2) was used for measurements of electron spectra. The spectrometer combines two different types of electron spectrometers, namely, integral one (a retarding sphere) and differential one (a double-pass cylindrical mirror energy analyzer). Several operation modes are available for the energy analysis of electron spectra. We applied the basic mode in which the retarding sphere (2) is grounded and the scanning retarding positive voltage (significantly affecting the spectrometer transmission) is put to the electron source (1). After passing the annular conic slit (3), the slowed-down electrons are affected by a constant negative analyzing voltage (defining the absolute instrumental resolution of the whole spectrometer) applied to the outer coaxial cylinder (5), whereas the inner cylinder (4) is grounded. Being delimited by four circular slits (3, 6) on the inner cylinder (4), the adjusted electron beam hits the windowless detector (a continuous channel electron multiplier) in the second focus (F2). Two lead absorbers (Pb) inside the inner cylinder protect the detector from the direct impact of the radiation emitted by electron sources.

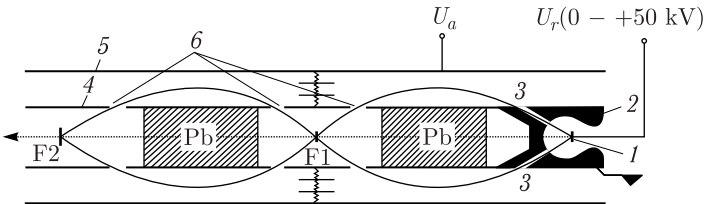


Fig. 2. A schematic view of the combined electrostatic electron spectrometer [14]: 1 – the electron source; 2 – the retarding sphere; 3 – the entrance annular conic slit; 4, 5 – the inner and outer coaxial cylindrical electrodes, respectively; 6 – the circular slits; F1, F2 – the first and the second focuses, respectively; Pb – the lead absorbers

In the present work, the spectra were measured in sweeps with scanning steps of 2 and 7 eV at absolute instrumental energy resolutions of 7 and 21 eV. Examples of the measured spectra are shown in Figs. 3–5.

The energy scale of the spectrometer was calibrated using 17 low-energy conversion electron lines (as specified below in parentheses). Twelve of them are related to the 8.41017(15) [15] ($M_{1,2}$, $N_{1,3}$), 20.74370(16) [15] (L_{1-3} , M_{1-3} , N_1), and 63.12044(3) keV [15] nuclear transitions in ^{169}Tm (created in the EC decay of ^{169}Yb , $T_{1/2} = 32.02$ d) and the other five are associated with the 14.41295(31) keV [16] nuclear transition in ^{57}Fe (K , L_{1-3} , M_1) arising from the EC decay of ^{57}Co ($T_{1/2} = 271.7$ d).

The energy of the individual calibration conversion line related to the Fermi level, $E_{F,i}^e$ (i is the line identification index), was evaluated applying Eq. (1) with the use of the experimental Fe and Tm electron binding energies $E_{F,i}^b$ [17] (also related to the Fermi level) and the energy E_γ of the relevant nuclear transition:

$$E_{F,i}^e = E_\gamma - E_{F,i}^b - E_{i,\text{rec}}^e. \quad (1)$$

The recoil kinetic energy $E_{i,\text{rec}}^e$ of atoms after emission of any calibration conversion electron was calculated to be well below 0.1 eV. In all cases

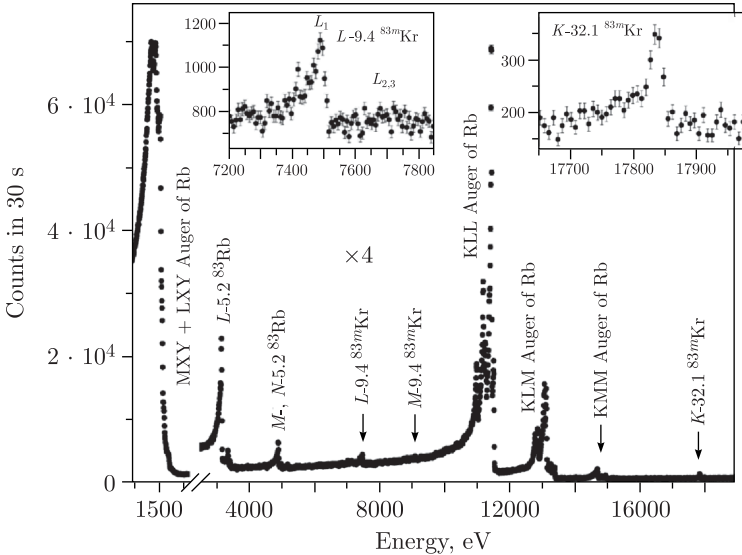


Fig. 3. An example of the measured overview low-energy electron spectrum emitted in the (EC + β^+) decay of ^{83}Sr ($T_{1/2} = 32.4$ d). The spectrum was taken with an instrumental energy resolution of 21 eV and a step of 7 eV. The exposition time per each spectrum point was 30 s. The spectrum was not corrected for the ^{83}Sr half-life as well as for the spectrometer transmission drop with increasing electron retardation voltage. In the inserts, the studied L -9.4 and K -32 conversion electron lines are shown in enlarged scales

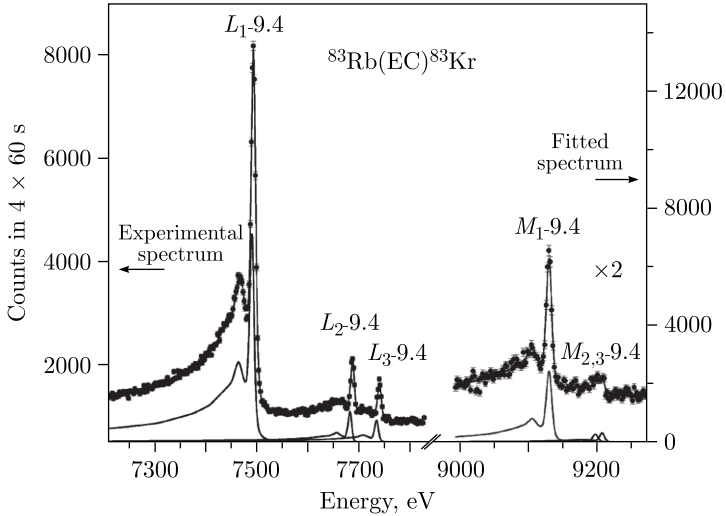


Fig. 4. An example of the measured L_{1-3} and M_{1-3} subshell conversion electron lines of the 9.4 keV nuclear transition in ^{83}Kr . The spectrum was taken at an instrumental resolution of 7 eV and a step size of 2 eV in four sweeps with an exposure time of 60 s per spectrum point in each sweep. Resulting spectrum components derived by the computer code [20] are shown by continuous lines

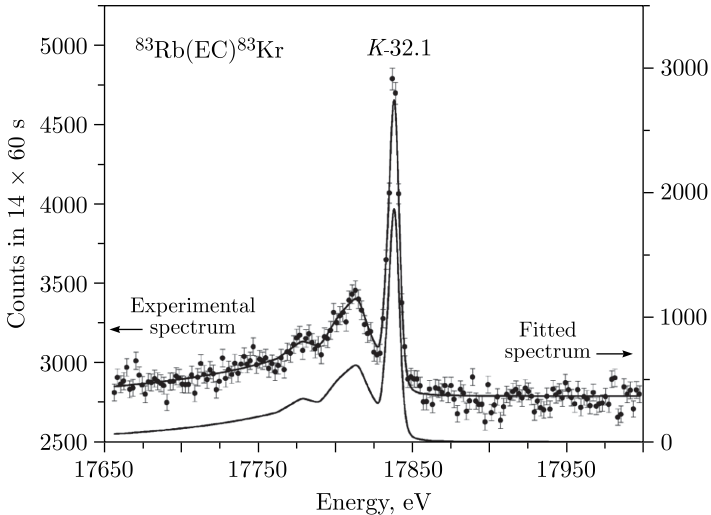


Fig. 5. An example of the K conversion electron line of the 32.1 keV nuclear transition in ^{83}Kr measured with an instrumental resolution of 7 eV and a step size of 2 eV in 14 sweeps with an exposure time of 60 s per spectrum point in each sweep. A resulting fit to the spectrum by the computer code [20] is shown by a continuous line

the $E_{F,i}^b$ uncertainties (from 0.4 to 0.9 eV for Fe and from 0.4 to 1.6 eV for Tm) dominate uncertainties of the above nuclear transition energies. Therefore, uncertainties of the evaluated calibration line energies were almost identical with those of the relevant electron binding energies. To ensure the local surrounding of the ^{169}Tm and ^{57}Fe atoms very close to that one at which the electron binding energy measurements [17] were performed, the calibration sources were prepared by vacuum evaporation on polycrystalline carbon backings [18]. Nevertheless, we found out that even changes of the Fe and Tm electron binding energies [17] within the maximum chemical shifts of about 2 (Fe) and 4 (Tm) eV measured in Ref. [19] for valence electrons affected the determined absolute electron energies (quoted in Tables 1–3 and in the text) negligibly compared with their stated standard deviations.

1.3. Spectra Processing. Applying the approach and the computer code SOFIE (see, e.g., Ref. [20]), the measured conversion electron spectra were decomposed into individual components. The spectral line profile was expressed by a convolution of the Lorentzian (describing the energy distribution of the investigated electrons leaving atoms) with an artificially created function based on the Gaussian. The purpose of the latter function is to describe both the response of the spectrometer to the monoenergetic electrons (the pure Gaussian) and the observed deformation of the measured conversion electron lines on their low-energy slopes. This deformation results from the inelastic electron scattering in the source material. It exhibits rather complicated structure and depends on many parameters. Some of them cannot be determined with the necessary precision in our case at present. Therefore, multiple fitting in the region of the energy losses for all evaluated spectral lines within the specified limits by the Monte Carlo procedure was applied in the method [20] to find out the adequate form of the conversion line deformation. In the spectra processing, the position and the height of each of the spectral lines and the linear background are the fitted parameters. The natural widths of the spectral lines and the width of the Gaussian (corresponding to the absolute spectrometer energy resolution) are usually fixed.

2. RESULTS AND DISCUSSION

2.1. Transition Energy Determination. From Eq. (1), one can derive the relation below for the determination of the energy value $E_{\gamma 9}$ of the 9.4 keV nuclear transition using the following quantities: i) the energy value $E_{\gamma 32}$ of the 32.1 keV nuclear transition, ii) the measured energy differences between the K -32 and the $L_{1,2,3}$ - and $M_{1,2,3}$ -9.4 conversion lines $\Delta E_{K32,i9}^e = (E_{F,K32}^e - E_{F,i9}^e)$, iii) the electron binding energies E_i^b in Kr atoms, and iv) the differences of the krypton atom recoil energies in the emission of the K -32 and the corresponding above-mentioned L - and M -9.4 conversion electrons $\Delta E_{K32,i9,\text{rec}}^e = (E_{K32,\text{rec}}^e - E_{i9,\text{rec}}^e)$:

$$E_{\gamma 9} = E_{\gamma 32} - (\Delta E_{K32,i9}^e - E_i^b) - E_K^b - \Delta E_{K32,i9,\text{rec}}^e. \quad (2)$$

Mutually independent are all values of $\Delta E_{K32,i9}^e$ as well as E_i^b . According to the calculations [21], the krypton atom recoil energies in the gas phase in the emission of the K -32 and the above L - and M -9.4 conversion electrons amount to 0.12, 0.051, and 0.061 eV, respectively, with the negligible uncertainties. Thus, the corresponding differences $\Delta E_{K32,i9,rec}^e$ of the krypton atom recoil energies should not be greater than 0.07 eV. Taking into account that in our case the ^{83}Kr atoms were bound in solid-state matrices, this value should be lower, i.e., negligible in comparison with other inaccuracies.

In our determination, the present value of 32151.6(5) eV [1] was used for the transition energy $E_{\gamma 32}$. The energy differences between the K -32 and the corresponding $L_{1,2,3}$ - and $M_{1,2,3}$ -9.4 keV conversion lines measured in the present work ($\Delta E_{K32,i9}^e$) are given in Table 1 (the 4th column). These values were obtained as weighted means of several independent measurements. Their numbers for particular $L_{1,2,3}$ - and $M_{1,2,3}$ -9.4 conversion lines are specified in the 3rd column of the table (NM). The electron binding energies in free Kr atoms, E_i^b , were taken from compilation [21] (denoted there as the

Table 1. The energy value $E_{\gamma 9}$ of the 9.4 keV ($M1 + E2$) nuclear transition in ^{83}Kr determined in the present work by the ICES method through the relation (2) and its comparison with the previous and present adopted values. See text for details

Subshell	E_i^b , eV	NM	$\Delta E_{K32,i9}^e$, eV	$\Delta E_{K32,i9}^e - E_i^b$, eV
K	14327.26(4)*			
L_1	1924.6(8)	6	10343.4(3)	8418.8(9)
L_2	1731.91(6)	4	10149.9(3)	8418.0(3)
L_3	1679.21(5)	4	10097.2(3)	8418.0(3)
M_1	292.74(29)	6	8710.6(3)	8417.9(44)
M_2	222.12(17)	4	8640.8(13)	8418.7(13)
M_3	214.54(11)	4	8632.0(10)	8417.5(10)
w.m.**				8418.0(2)
Current results for $E_{\gamma 9} = E_{\gamma 32} - \text{w.m.}(\Delta E_{K32,i9}^e - E_i^b) - E_K^b$				
$E_{\gamma 9}$ [3]				9405.9(8)
$E_{\gamma 9}$ [2]				9396(3)
$E_{\gamma 9}$ [4]				9405.8(3)
Our value				9406.3(5)
w.m. (previous [2-4] and our results)				9405.9(5)
w.m. (previous [3, 4] and our results)				9405.9(5)
Present adopted value [1]				9405.7(6)
$E_{\gamma 32} - E_{\gamma 9} = \text{w.m.}(\Delta E_{K32,i9}^e - E_i^b) + E_K^b$				22745.3(2)
* 14327.26(4) means 14327.26 ± 0.04 .				
** w.m. means the weighted mean.				

“adopted weighted mean values”). They are displayed in the 2nd column of the table.

Using a weighted mean of six independent values of $\Delta E_{K32,i9}^e$, the transition energy $E_{\gamma 9} = 9406.3(5)$ eV was obtained. As can be seen from Table 1, this value agrees very well (within 1σ) with the above-mentioned values [3, 4], but is higher by more than 3σ than the result of the previous analogous measurement [2]. Equation (2) enabled us to determine also the energy difference $E_{\gamma 32} - E_{\gamma 9} = 22745.3(2)$ eV directly from our experimental data (the last row of the table).

In Table 2, the energy differences $\Delta E_{K32,i9}^e$ from the previous investigation [2] (not published until now) are compared with our values. As can be seen, they are all greater by a weighted mean (w.m.) value of 1.4(8) eV than ours. Using the previous [2] $\Delta E_{K32,i9}^e$ values, the differences $\Delta E_{K,i}^b$ of the electron binding energies in free Kr atoms [21] (used in the present work) and the actual value $E_{\gamma 32} = 32151.6(5)$ eV [1], a new value of the transition energy $E_{\gamma 9} = 9404.7(7)$ eV was derived through Eq. (2) (see lower part of the table). This value is lower only by 1.6(8) eV than our one. This analysis indicates that the main influence on the determination of the transition energy $E_{\gamma 9}$ in the previous work [2] had the chosen set of the electron binding energies in free Kr atoms and the value of the transition energy $E_{\gamma 32}$ used.

Table 2. A comparison of the energy differences $\Delta E_{K32,i9}^e$ between the K-32 and the $L_{1,2,3}$ - and $M_{1,2,3}$ -9.4 keV conversion lines measured in the present work with those of the previous investigation [2]. Corresponding differences are given in the 3rd row

Energy	Subshell				
	$\Delta(K, L_1)$	$\Delta(K, L_2)$	$\Delta(K, L_3)$	$\Delta(K, M_1)$	$\Delta(K, N_1)$
$\Delta E_{K32,i9}^e$ [2]	10345.2(15)*	10151.2(15)	10098.4(15)	8711.8(15)	8447.6(15)
$\Delta E_{K32,i9}^e$ (t.w.)**	10343.4(3)	10149.9(3)	10097.2(3)	8710.6(33)	
$\Delta E_{K32,i9}^e$ [2] – t.w.	+ 1.8(15)	+ 1.3(15)	+ 1.2(15)	+ 1.2(15)	
w.m.*** ([2] – t.w.)	+ 1.4(8)				
$\Delta E_{K32,i9}^e$ [2] – E_i^b [21]	8420.6(17)	8419.3(15)	8419.2(15)	8419.1(15)	8420.1(15)
w.m. ($\Delta E_{K32,i9}^e - E_i^b$)	8419.62(69)				
$E_{\gamma 9} = E_{\gamma 32} - \text{w.m.}$ ($\Delta E_{K32,i9}^e - E_i^b$) – E_K^b	9404.7(9)				
$E_{\gamma 9}$ (t.w.)	9406.3(5)				
$E_{\gamma 9}$ (t.w.) – $E_{\gamma 9}$ ([2])	1.6(10)				
* 10345.2(1.5) means 10345.2 ± 1.5 .					
** t.w. means this work.					
*** w.m. means the weighted mean.					

2.2. Electron Binding Energies in Kr in Different Solid-State Matrices.

Using the energies of the K -32, L_{1-3} -9.4, and M_{1-3} -9.4 conversion lines (related to the Fermi level) measured in the present work with the ^{83}Sr sources prepared by ion implantation into the polycrystalline Pt foil (see the 1st row of Table 3, $E_{F,i,\text{impl}}^e$) and the nuclear transition energies $E_{\gamma,9} = 9405.8(3)$ eV (the weighted mean of the values [3,4]) and $E_{\gamma,32} = 32151.6(5)$ eV [1], we determined the electron binding energies (related to the Fermi level) in Kr in this matrix on the relevant subshells by means of Eq. (1). The krypton atom recoil energies in the gas phase in the emission of the K -32, L_{1-3} -9.4 and M_{1-3} -9.4 conversion electrons [21], amounting to 0.12, 0.051, and 0.061 eV, respectively, were also taken into account. The obtained values of $E_{F,i,\text{impl}}^b$ are presented in Table 3 in the 2nd row. In the next row, the electron binding energies in free Kr atoms (“adopted weighted mean values”) [21] are also given. As can be seen from the table (the 5th row, w.m. (ΔE_i^b)), the electron binding energies in free Kr atoms in investigated subshells are greater by a weighted mean value of 11.6(4) eV. A significant deal of this difference is due to the work function of platinum as the electron binding energies in free Kr atoms [21] are referenced to the vacuum level. According to different publications, the work function of platinum ranges from 4.6 to 6.4 eV. In the work [22] it was derived that the electron binding energy in the M_3 subshell of Kr implanted into the polycrystalline Pt should be lower even by 7.5 eV than in the case of free Kr atoms. It is generally known that the work function depends on both the properties of the metal and the nature of its surface, and is strongly affected by the condition of the surface. However, in our investigation the source surfaces were not purposefully cleaned before the measurements. In Ref. [23], the binding energies of core electrons of Ne, Ar, Kr, and Xe implanted into polycrystalline Cu, Ag, and Au matrices were measured by X-ray photoemission. After their correction for work functions of the substrates, they were found to be smaller by 2–4 eV than the corresponding binding energies obtained from gas-phase measurements. Unfortunately, the data on Kr implanted into Au matrix were not obtained. Nevertheless, it was found that for the given rare gas the above-mentioned shift of the core electron binding energy is largest in Ag and smallest in Cu. Thus, taking into account both the above work function value of 7.5 eV [22] and the additional energy shift from 2 to 4 eV [23] caused by some solid-state effects, lowering of the studied electron binding energies in Kr in our implanted ^{83}Sr sources by 11.6(4) eV can be explained.

From the energies of the K -32, L_{1-3} -9.4, and M_{1-3} -9.4 conversion lines measured in the present work with the ^{83}Rb source prepared by vacuum evaporation on the polycrystalline Pt foil, shifts of the electron binding energies in Kr in such a source in comparison with those of the implanted ^{83}Sr sources were derived. (Not to overload Table 3 with data, we do not display them.) The binding energies in question were found to be lower by the weighted mean value of 2.9(2) eV (see the middle of Table 3 — $\Delta E_{F,i}^b$ (impl, Pt – evap, Pt)).

Table 3. A comparison of the electron binding energies (related to the Fermi level) in Kr implanted into a Pt matrix ($E_{F,i,\text{impl}}^b$) and situated in evaporated layers on Pt and Al substrate. All energy values are given in eV

Energy	Subshell							
	K	L_1	L_2	L_3	M_1	M_2	M_3	
$E_{F,i,\text{impl}}^c$	17835.8(8)*	7491.4(7)	7685.3(8)	7738.2(8)	9124.3(8)	9196.2(11)	9204.6(14)	
$E_{F,i,\text{impl}}^b$	14315.7(9)	1914.4(8)	1720.4(8)	1667.6(8)	281.4(9)	209.5(11)	201.1(14)	
$E_{F,i,\text{free}}^b$ [21]	14327.26(4)	1924.6(8)	1731.91(6)	1679.21(5)	292.74(29)	222.12(17)	214.54(11)	
ΔE_2^b (free – impl, Pt)	11.6(9)	10.3(11)	11.5(8)	11.6(88)	11.3(9)	12.6(12)	13.4(14)	
w.m.** (ΔE_i^b)	11.6(4)							
w.m. ($\Delta E_{F,i}^b$) (impl, Pt – evap, Pt)	2.9(2)							
$E_{F,i,\text{evap,Al}}^c$ [2]	17834.7(11)	7489.4(10)	7683.5(10)	7736.3(10)	9122.9(10)			
$\Delta E_{F,i}^b$ (evap, Al – impl, Pt)	1.1(13)	2.0(12)	1.8(13)	1.9(13)	1.4(13)			
w.m. ($\Delta E_{F,i}^b$)	1.7(6)							

*17835.8(8) means 17835.8 ± 0.8 .

**w.m. means the weighted mean.

In the lower part of Table 3, the energies of the K -32, L_{1-3} -9.4, and M_1 -9.4 conversion lines measured in the previous work [2] (not yet published) with an ^{83}Rb source prepared by vacuum evaporation on the polycrystalline Al foil are given. As can be seen from the table, the binding energies in Kr in such a matrix are surprisingly greater by a weighted mean value of 1.7(6) eV than those for Kr implanted into the polycrystalline Pt foil. The backing material (not pure Al but insulator Al_2O_3) could contribute to this effect.

CONCLUSION

The ICES method developed by the authors for several decades enabled one to determine the energy of the 9.4 keV ($M_1 + E_2$) nuclear transition in ^{83}Kr with high precision despite limitations caused by precision of other inevitable data. Our investigation again demonstrates that the ICES method remains a powerful tool for accurate determination of not only nuclear transition energies particularly in the low energy region, but also of other physical quantities.

Acknowledgements. The authors are indebted to M. Ryšavý for the careful revision of the manuscript.

REFERENCES

1. *McCutchan E. A.* // Nucl. Data Sheets ($A = 83$). 2015. V. 125. P. 201.
2. *Kovalík A., Gorozhankin V. M.* // J. Phys. G: Nucl. Part. Phys. 1993. V. 19. P. 1921; DOI:10.1088/0954-3899/19/11/018.
3. *Picard A., Backe H., Bonn J., Degen B., Haid R., Hermann A., Leiderer P., Osipowicz A., Otten E. W., Przyrembel M., Schrader M., Steininger M., Weinheimer Ch.* // Z. Phys. A: Hadr. Nucl. 1992. V. 342. P. 74; DOI:10.1007/BF01294491.
4. *Slezák M., Vénos D., Lebeda O., Trojek T.* // Eur. Phys. J. A. 2012. V. 48. P. 12; DOI 10.1140/epja/i2012-12012-y.
5. *Inoyatov A. Kh., Ryšavý M., Kovalík A., Filosofov D. V., Zhdanov V. S., Yushkevich Yu. V.* // Eur. Phys. J. A. 2012. V. 50. V. 59; DOI 10.1140/epja/i2014-14059-0.
6. *Inoyatov A. Kh., Kovalík A., Perevoshchikov L. L., Filosofov D. V., Vénos D., Lee B. Q., Ekman J., Baimukhanova A.* // J. Phys. B: At. Mol. Opt. Phys. 2017. V. 50. P. 155001; DOI: 10.1088/1361-6455/aa7990.
7. *Ziegler J.* Software Package SRIM. <http://www.srim.org/>, 2011.
8. *Špalek A.* // Surf. Interface Anal. 1990. V. 15. P. 739; DOI: 10.1002/sia.740151206.
9. *Vénos D., Zbořil M., Kašpar J., Dragoun O., Bonn J., Kovalík A., Lebeda O., Lebedev N. A., Ryšavý M., Schlösser K., Špalek A., Weinheimer Ch.* // Meas. Tech. 2010. V. 53. V. 573.
10. *Zbořil M., Bauer S., Beck M., Bonn J., Dragoun O., Jakůbek J., Johnston K., Kovalík A., Otten E. W., Schlösser K., Slezák M., Špalek A., Thümmel T., Vénos D., Žemlička J., Weinheimer Ch.* // J. Instrum. 2013. V. 8. P. 03009; DOI: 10.1088/1748-0221/8/03/P03009.

11. Fižer M., Brabec V., Dragoun O., Kovalík A., Frana J., Ryšavý M. // Intern. J. Appl. Radiat. Isot. 1985. V. 36. P. 219.
12. Gerasimov V.N., Zelenkov A.G., Kulakov V.M., Pchelin V.A., Soldatov A.A., Chistyakov L.V. // Yad. Fiz. 1981. V. 34. P. 3.
13. Gerasimov V.N., Zelenkov A.G., Kulakov V.M., Pchelin V.A., Sokolovskaya M.V., Soldatov A.A., Chistyakov L.V. // Zh. Eksp. Teor. Fiz. 1982. V. 82. P. 362; JETP. 1982. V. 55. P. 205.
14. Briançon Ch., Legrand B., Walen R.J., Vylov Ts., Minkova A., Inoyatov A. // Nucl. Instr. Meth. 1984. V. 221. P. 547; DOI: 10.1016/0167-5087(84)90062-0.
15. Baglin C.M. // Nucl. Data Sheets for $A = 169$. 2008. V. 109. P. 2033; DOI: 10.1016/j.nds.2008.08.001.
16. Update of X Ray and Gamma Ray Data Standards for Detector Calibration and Other Applications. V.1 // Recommended Decay Data, High Energy Gamma Ray Standards and Angular Correlation Coefficients. Vienna: Int. Atomic Energy Agency, 2007. P. 12.
17. Sevier K.D. // Atom. Data Nucl. Data Tables. 1979. V. 24. P. 323; DOI: 10.1016/0092-640X(79)90012-3.
18. Inoyatov A. Kh., Kovalík A., Filosofov D. V., Yushkevich Yu. V., Ryšavý M., Zbořil M. // J. Electron Spectrosc. Relat. Phenom. 2015. V. 202. P. 46; DOI: 10.1016/j.elspec.2015.02.015.
19. Naumkin A. V., Kraut-Vass A., Gaarenstroom S. W., Powell C.J. NIST Standard Reference Database 20, Version 4.1. X-Ray Photoelectron Spectroscopy Database. <http://srdata.nist.gov/xps/selEnergyType.aspx>.
20. Inoyatov A., Filosofov D. V., Gorozhankin V. M., Kovalík A., Perevoshchikov L. L., Vylov Ts. // J. Electron Spectrosc. Relat. Phenom. 2007. V. 160. P. 54; DOI: 10.1016/j.elspec.2007.06.005.
21. Vénos D., Sentkerestiová J., Dragoun O., Slezák M., Ryšavý M., Špalek A. // J. Instrum. 2018. V. 13, No. 02. P. T02012.
22. Zbořil M. Solid Electron Sources for the Energy Scale Monitoring in the KATRIN Experiment. PhD Thesis. Westfälische Wilhelms-Universität Muenster, 2011.
23. Citrin P. H., Hamann D. R. // Phys. Rev. B. 1974. V. 10. P. 4948.

Received on December 19, 2022.

Редактор *Е. И. Кравченко*

Подписано в печать 08.02.2023.

Формат 60 × 90/16. Бумага офсетная. Печать цифровая.

Усл. печ. л. 0,75. Уч.-изд. л. 0,97. Тираж 120 экз. Заказ № 60563.

Издательский отдел Объединенного института ядерных исследований
141980, г. Дубна, Московская обл., ул. Жолио-Кюри, 6.

E-mail: publish@jinr.ru

www.jinr.ru/publish/